Supporting Information

*Adriele A. de Almeida[1], Emilio De Biasi[1,2], Marcelo Vasquez Mansilla[1], Daniela P. Valdés[1,2], Horacio E. Troiani[2,3], Guillermina Urretavizcaya[4], Teobaldo E. Torres[1], Luis M. Rodríguez[1], Daniel E. Fregenal[5], Guillermo C. Bernardi[1], Elin L. Winkler[1,2], Gerardo F. Goya[6,7], Roberto D. Zysler[1,2], Enio Lima Jr.[1,]**

Magnetic Hyperthermia Experiments with $Zn_xFe_{3-x}O_4$ Nanoparticles in Clarified Butter Oil and Paraffin: a Thermodynamic Analysis

[1] Instituto de Nanociencia y Nanotecnología, CNEA-CONICET, Centro Atómico Bariloche, S. C. de Bariloche, 8400, RN, Argentina.

[2] Instituto Balseiro, CNEA-UNCuyo, Centro Atómico Bariloche, S. C. de Bariloche, 8400, RN, Argentina.

[3] Lab. de Caracterización de Materiales y Óxidos No-Estequiométricos, Gerencia de Investigación Aplicada, Centro Atómico Bariloche, S. C. de Bariloche, 8400, RN, Argentina.

[4] Consejo Nacional de Investigaciones Científicas y Técnicas (CONICET) e Instituto Balseiro, Centro Atómico Bariloche, S. C. de Bariloche, 8400, RN, Argentina.

[5] Centro Atómico Bariloche, Bustillo 9500, San Carlos de Bariloche, 8400, Río Negro, Argentina

[6] Dep. de Física de la Materia Condensada, Universidad de Zaragoza, Mariano Esquillor s/n, Zaragoza, 50018, Spain.

[7] Instituto de Nanociencia de Aragón, Universidad de Zaragoza, Mariano Esquillor s/n, Zaragoza, 50018, Spain.

* author to whom correspondence: lima@cab.cnea.gov.ar

Content: 12 pages; 10 figures

Compositional analysis of the four samples with Proton Induced X-ray Emission (PIXE).

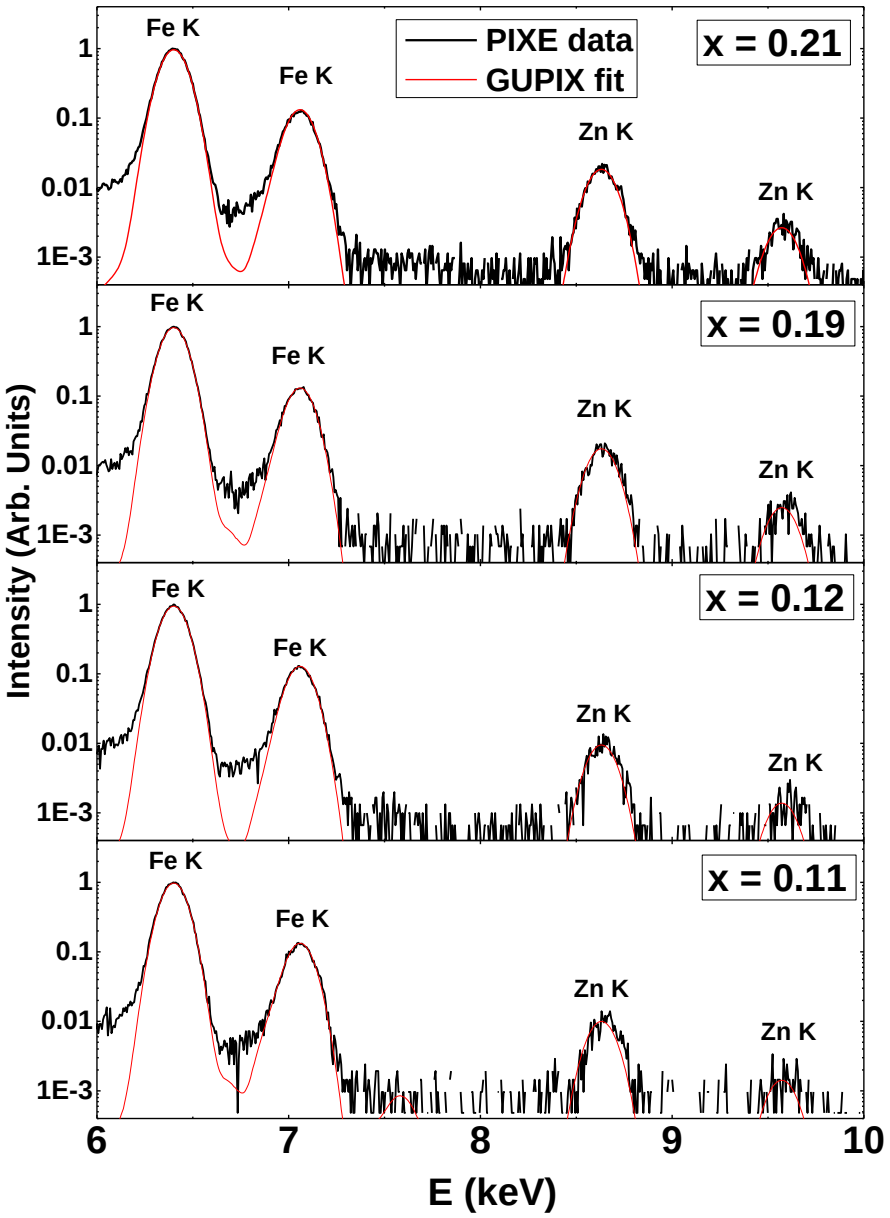

Figure S1: PIXE results in the Fe and Zn K-band energy range (black lines) and the corresponding peak fits with GUPIX (red lines).

X-ray diffraction (XRD) measurements of sample X=0.21 as representative of the samples.

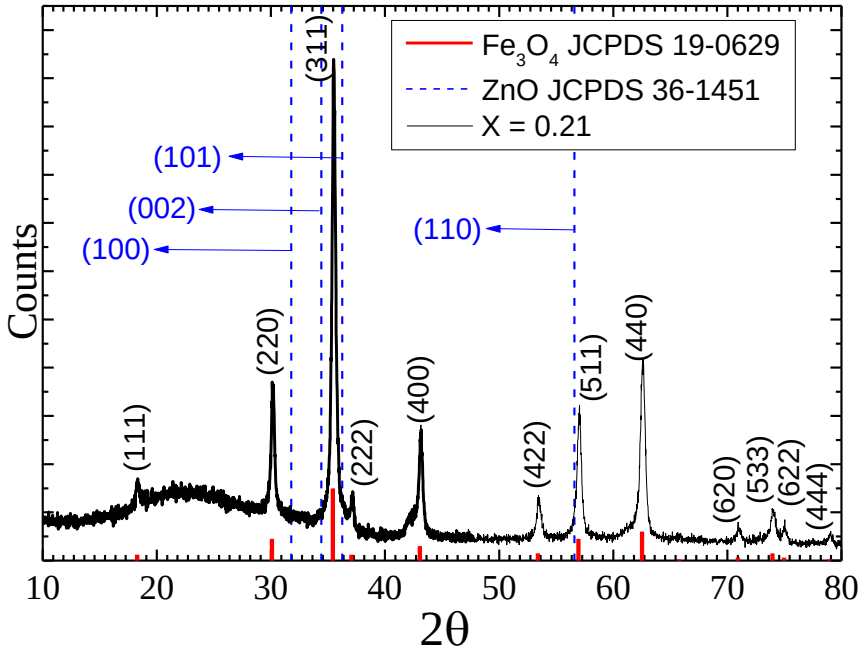

Figure S2: XRD profile of sample x=0.21, where the diffraction peaks observed can be addressed to the cubic magnetite phase (JCPDS card 19-0629, red bars at the bottom part of the graphic). No evidence of the ZnO phase is observed in the limit of our background and peak width, as indicated by the absence of diffraction in the positions expected for the most intense peaks (dashed blue lines) of the hexagonal ZnO phase (JCPDS card 36-1451).

Saturation Magnetization (M_S) determined by from the magnetic measurements (M(H) curves).

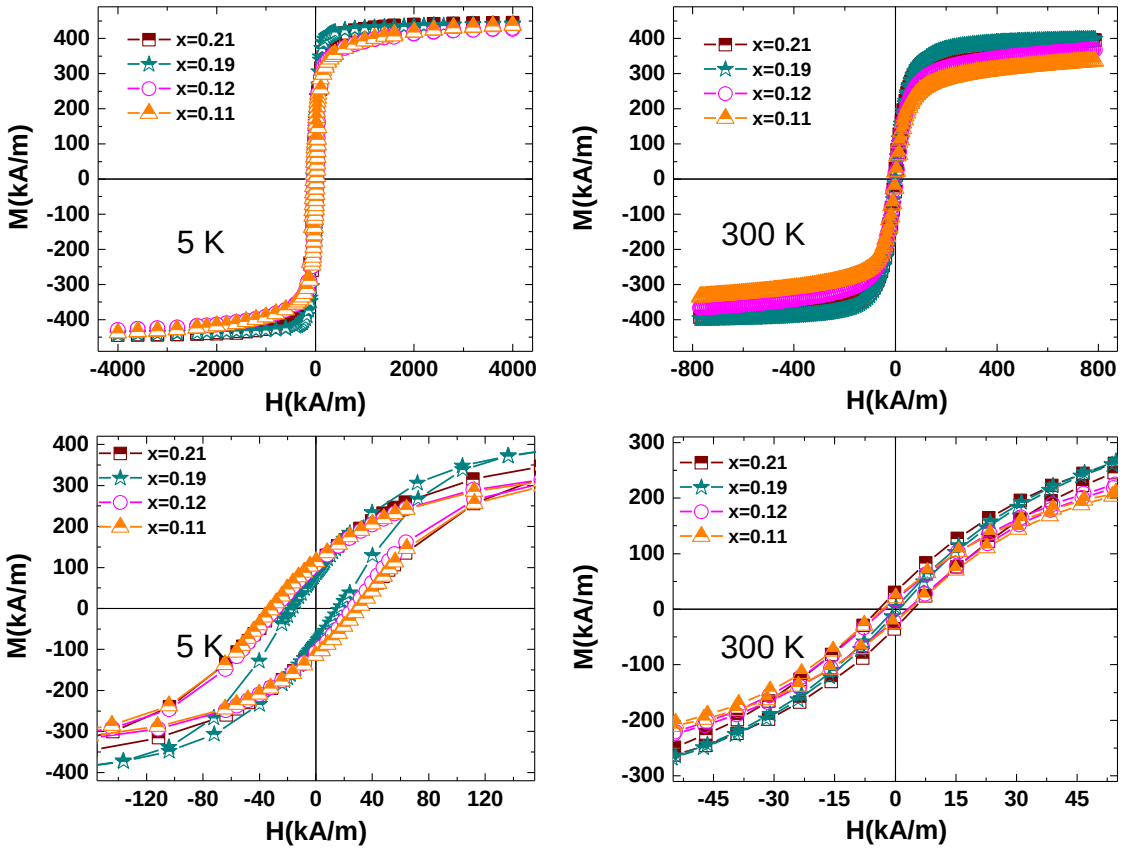

Figure S3: Top panel gives M(H) curves of all samples measured at (a) 5 K measured in SQUID magnetometer and (b) 300 K measured in a VSM. Bottom panel shows the low-field region of the respective curves.

Obtaining the blocking-temperature distribution $f(T_B)$ from the magnetization measurements as function of temperature ($M_{ZFC}(T)$ and $M_{FC}(T)$)

The distribution of energy barrier and consequently the volume distribution of a system constituted by single-domain nanoparticles can be obtained, under certain conditions, from the magnetization curves as a function of temperature (*M(T)*) measured with zero-field-cooling (ZFC) and field-cooling (FC) protocols.

Firstly, we consider non-interacting or very weakly interacting nanoparticles so that the energy barrier can be assumed proportional to the volume of the single-domain, $\Delta E=K.v$, and assuming that the anisotropy constant K is the same for all particles. Taking these conditions, the blocking temperature T_B is proportional to the volume v of the particle: $T_B=\alpha v$, where α is a parameter that depends on the ratio between the measurement time and the relaxation time at infinite temperature, as well as on the anisotropy constant (assuming a uniaxial anisotropy and a very weak external field with respect to the anisotropy field of the particle).

In this way, the description of the magnetization curve of a particle of a given volume v measured under ZFC conditions ($M_{ZFC}(T)$) corresponds to a Curie's law for temperatures greater than its blocking temperature, that is:

$$M_{ZFC}(T) = \frac{\mu^2 H}{3\,k_B}\left\{\frac{1}{T}\theta\big(T - T_B(v)\big)\right\}, \quad (1)$$

where $\mu=M_S.v$ is the single-domain magnetic moment and $\theta(x)$ is the step distribution.

In the same way, the description of the magnetization curve of this same particle measured under FC conditions ($M_{FC}(T)$) corresponds to the Curie's law for temperatures higher than its blocking temperature, and for temperatures lower than T_B, the magnetization is constant and equal to $M(T_B)$:

$$M_{FC}(T) = \frac{\mu^2 H}{3\,k_B}\left\{\frac{1}{T_B(v)}\,\theta(T_B(v) - T) + \frac{1}{T}\theta\big(T - T_B(v)\big)\right\} \quad (2)$$

In a real nanoparticle system, there is a volume distribution, f(v), which must be integrable in the volume interval and null at infinity. In this way, the magnetization curves (M(T)) that include the volume distribution are expressed as:

$$M_{ZFC}(T) = \frac{M_S^2 H}{3\,k_B}\int_0^\infty \frac{v^2}{T}\theta\big(T - T_B(v)\big)f(v)dv \quad (3)$$

$$M_{FC}(T) = \frac{M_S^2 H}{3\,k_B}\int_0^\infty \frac{v^2}{T}\theta\big(T - T_B(v)\big)f(v)dv + \frac{M_S^2 H}{3\,k_B}\int_0^\infty v.\theta(T_B(v) - T)f(v)dv. \quad (4)$$

In this way, the quantity $\Delta(T)=M_{ZFC}(T)-M_{FC}(T)$ for a single-domain particle system with a size distribution $f(v)$ is given by:

$$\Delta(T) = -\frac{{M_s}^2 H}{3\,k_B}\int_0^\infty v\,\theta(T_B(v) - T)\,f(v)\;dv \quad (5)$$

$$\Delta(T) = -\frac{{M_s}^2 H}{3\,k_B}\int_{v(T)}^\infty v\,f(v)\;dv = \frac{{M_s}^2 H}{3\,k_B}G(T), \quad (6)$$

where $\Delta(T)=M_{ZFC}(T)-M_{FC}(T)$ is null in the upper integration limit and the lower integration limit $v(T)$ is the volume of the single-domain that blocks at the temperature T. In addition, $G(T)$ satisfies:

$$\frac{dG(T)}{dv} = v(T)f(v(T)). \quad (7)$$

Differentiating ΔT with respect to T and remembering that $v(T)=T/\alpha$, we obtain:

$$\frac{d\,\Delta(T)}{d\,T} = \frac{d\,\Delta(T)}{d\,v}\,\frac{d\,v}{d\,T} = \frac{{M_s}^2 H}{\alpha 3\,k_B}\frac{T}{\alpha} f\left(\frac{T}{\alpha}\right), \quad (8)$$

or

$$\frac{1}{T}\frac{d\,\Delta(T)}{d\,T} = \frac{{M_s}^2 H}{\alpha^2 3\,k_B} f\left(\frac{T}{\alpha}\right). \quad (9)$$

Different methods are used in order to determine the blocking temperature distribution $f(T_B)$, as exemplified in references [1-5]. The difference between the $f(T_B)$ obtained by these methods depends on the dispersion of the size distribution, being small for the dispersion normally obtained by our synthesis method. However, when large particles are present in the sample, their population can be overestimated in some cases due to their large magnetic moment.

As several works used the expression $d(M_{ZFC}-M_{FC})/dT$ in order to obtain the blocking temperature distribution, we compare in figure SI4(a) the distributions obtained for our samples by the later expression ($f^{+}(T_B)$) and that used by us (eq. (9)). As observed, the main peak referent to the blocking process is not so different between then. However, contributions at higher temperatures is larger when using $d(M_{ZFC}-M_{FC})/dT$, resulting in a larger mean blocking temperature at the same time the Verwey transition is highlighted for sample x=0.21. Despite these differences, both $<T_B>$ values indicate a Neel relaxation time smaller, at least about 10 times, than the Brown one in the temperature range (above 310 K) where the CBO present low-viscosity (figure S4(b)). In this way, the analysis of hyperthermia results should not be affected by using these two methods to determine the blocking temperature distribution.

[1] H. Mamiya, M. Ohnuma, I. Nakatani and T. Furubayashim. Extraction of blocking temperature distribution from zero-field-cooled and field-cooled magnetization curves. IEEE T. Magn. **41**, 3394 (2005).

[2] D. A. Balaev, S. V. Semenov, A. A. Dubrovskiy, S. S. Yakushkin, V. L. Kirillov, O. N. Martyanov. Superparamegntic blocking in an ensemble of magnetite nanoparticles upon interparticle interactions. J. Magn. Magn. Mater. **440**, 199 (2017).

[3] N. A. Usov. Numerical simulation of field-cooled and zero field-cooled processes for assembly of superparamagnetic nanoparticles with uniaxial anisotropy. J. Appl. Phys. **109**, 023913 (2011).

[4] K. L. Livesey, S. Ruta, N. R. Anderson, D. Baldomir, R. W. Chantrell and D. Serantes. Beyond the blocking model to fit nanoparticle ZFC/FC magnetization curves. Sci. Rep. **8**, 11166 (2018).

[5] G. Muscas, G. Concas, S. Laureti, A. M. Testa, R. Mathieu, J. A. De Toro, C. Cannas, A. Musinu, M. A. Novak, C. Sangregorio, Su Seong Lee and D. Peddis. The interplay between single particle anisotropy and interparticle interactions in ensembles of magnetic nanoparticles. Phys. Chem. Chem. Phys. **20**, 28634 (2018).

Blocking temperature distributions obtained from $M_{ZFC}(T)$ and $M_{FC}(T)$ curves of all samples obtained by $(1/T)d(M_{ZFC}-M_{FC})/dT$ and $d(M_{ZFC}-M_{FC})/dT$ ($f(T_B)$ and $f^+(T_B)$, respectively) and Relaxation times diagram calculated considering the blocking temperature obtained from each distribution.

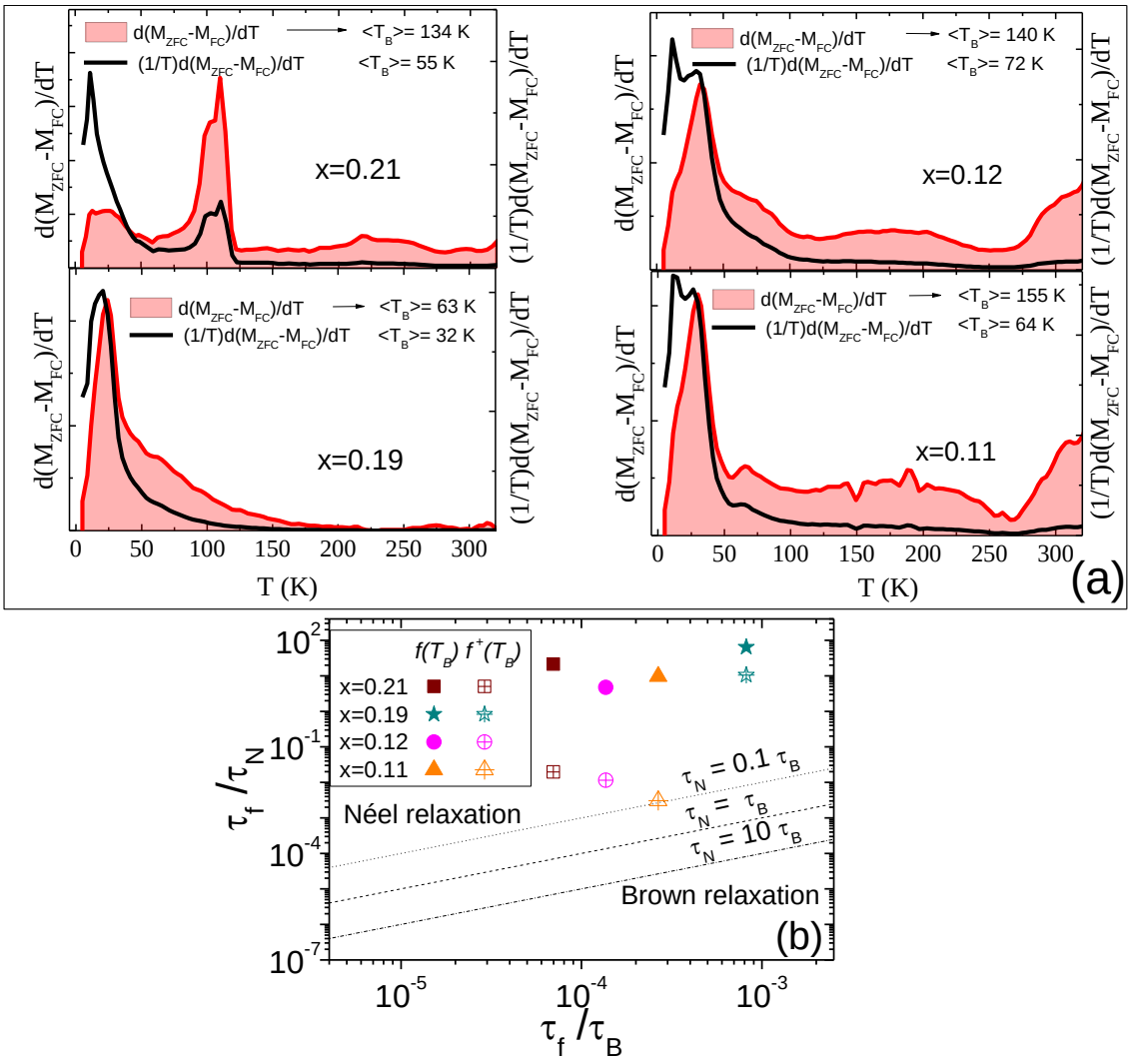

Figure S4: (a) Blocking temperature distributions obtained from $M_{ZFC}(T)$ and $M_{FC}(T)$ curves of all samples obtained by $(1/T)d(M_{ZFC}-M_{FC})/dT$ and $d(M_{ZFC}-M_{FC})/dT$ ($f(T_B)$ and $f^+(T_B)$, respectively). (b) Relaxation times diagram where the Néel (τ_N) and Brown (τ_B) relaxation times of the different nanoparticles dispersed in CBO normalized by the applied field period ($\tau_f = 1/(2\pi f)$) are plotted; later data were calculated for the temperature of 312 K, where the CBO presents low viscosity, from the mean blocking temperatures obtained from figure S4(a).

Magnetization as function of applied field (M(H) curves) measured in VSM for CBO and paraffin without nanoparticles at 300 K.

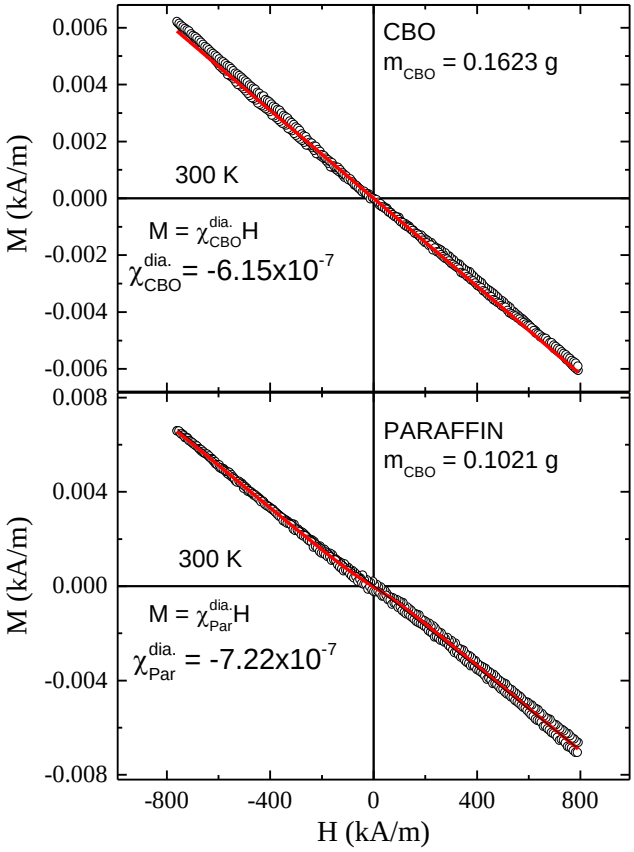

Figure S5 – M(H) curves at 300 K (open circles) of CBO (top panel) and paraffin (bottom panel) without nanoparticles. Solid red line gives the fit with a diamagnetic function for both samples, indicating the absence of magnetic contaminations in the limit of detection.

Magnetic Fluid Hyperthermia measurements of CBO and Paraffin without Nanoparticles performed in the F1-D5 -model.

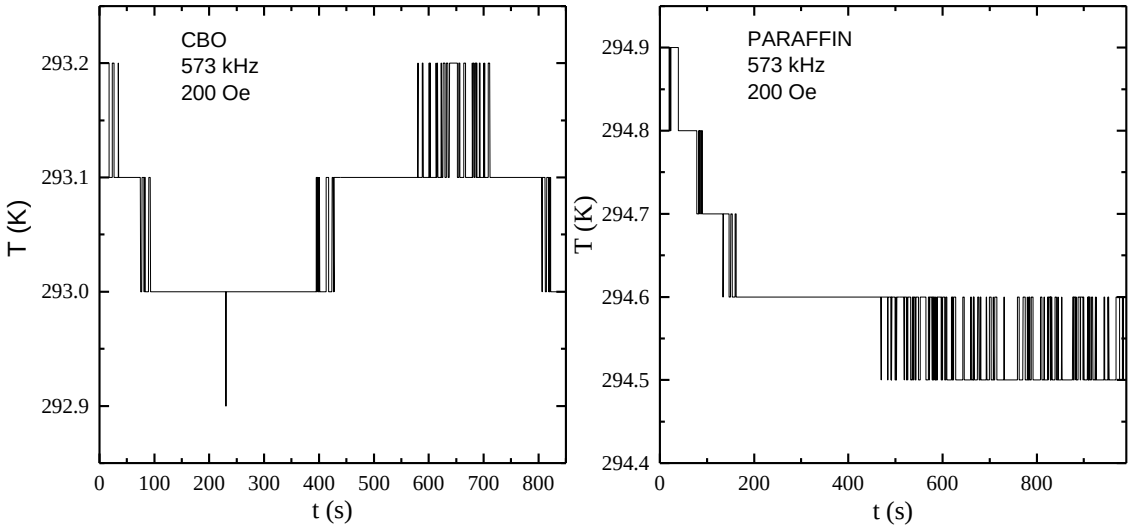

Figure S6: Temperature increment as function of time for CBO and paraffin without Nanoparticles, showing the absence of temperature increment without the magnetic nanoparticles during the time interval typical of hyperthermia experiments.

Changes in the physical aspects of Clarified Butter Oil (CBO) with the temperature, which is related with the changes in the viscosity and specific heat.

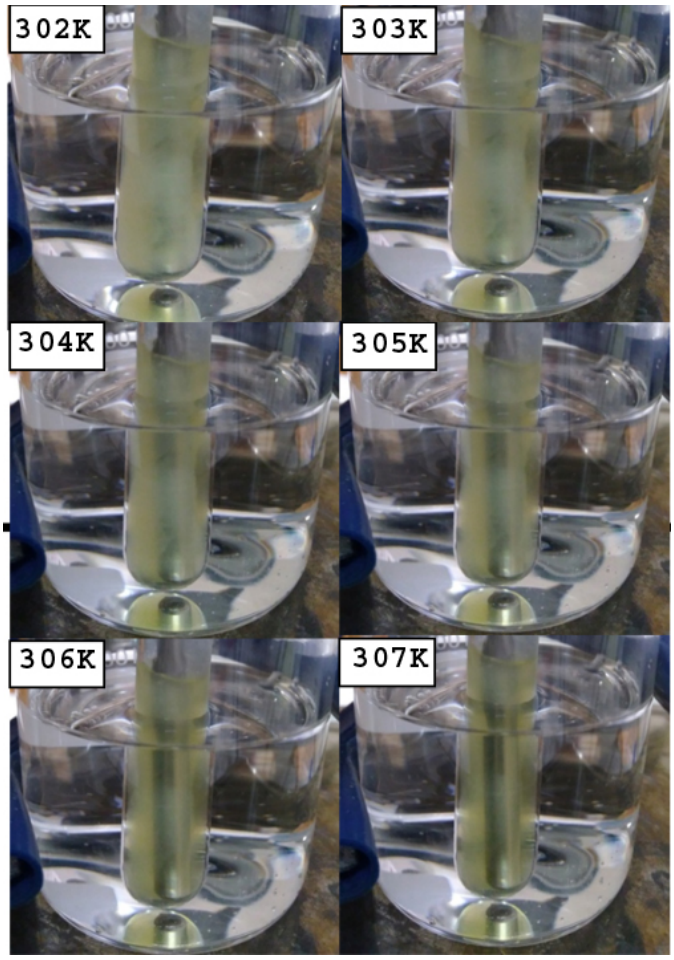

Figure S7 – Photography of CBO taken at the specified temperature.

Cooling curve of CBO+NPs heated in a hot plate up to a temperature above the melting taken in the DM100-model and its analysis with respect to the quantity $\boldsymbol{\Gamma = \int_{t_0}^{t} c_P(T)\left(\frac{dT}{dt}\right) dt}$ ***in order to estimate*** $\boldsymbol{\Delta Q_{loss}}$.

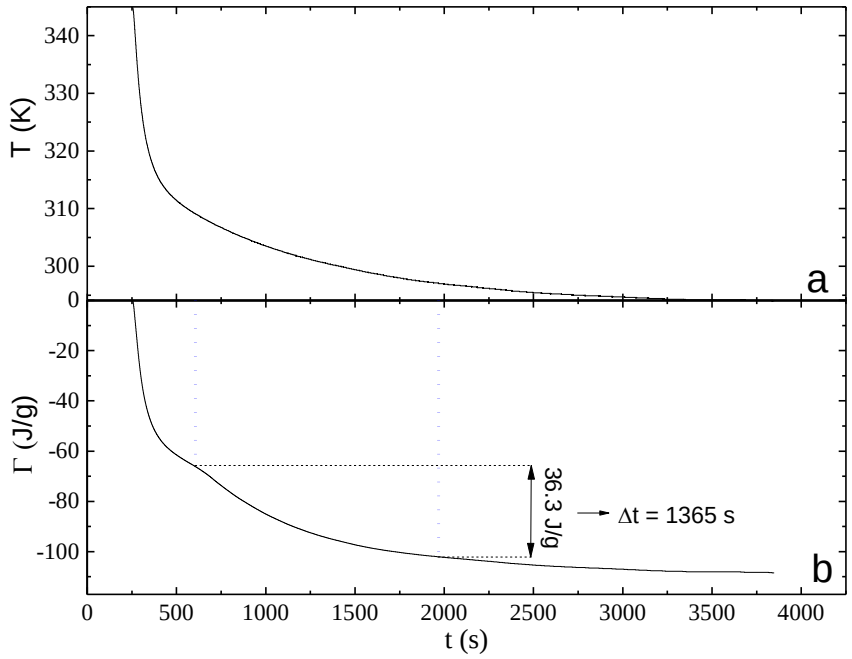

Figure S8: (a) Cooling curve of CBO+NPs heated in a hot plate up to a temperature above the melting taken in the DM100-model and (b) its analysis with respect to the quantity $\Gamma = \int_{t_0}^{t} c_P(T)\left(\frac{dT}{dt}\right) dt$ in order to estimate ΔQ_{loss} between T_i and T_F interval that defines the HFM melting of the CBO.

Cooling curve of Paraffin+NPs heated in a hot plate up to a temperature above the melting taken in the D5-F1-model and its analysis with respect to the quantity $\boldsymbol{\Gamma = \int_{t_0}^{t} c_P(T)\left(\frac{dT}{dt}\right) dt}$ ***in order to estimate*** $\boldsymbol{\Delta Q_{loss}}$.

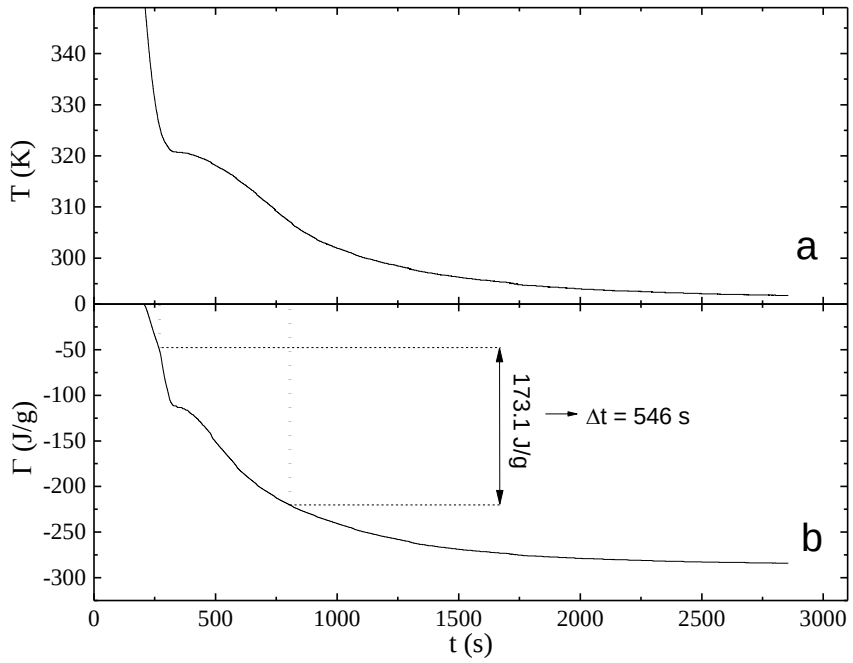

Figure S9: (a) Cooling curve of Paraffin+NPs heated in a hot plate up to a temperature above the melting taken in the D5-F1-model and (b) its analysis with respect to the quantity $\Gamma = \int_{t_0}^{t} c_P(T)\left(\frac{dT}{dt}\right) dt$ in order to estimate ΔQ_{loss} between T_i and T_F interval that defines the melting of the Paraffin.

Magnetic Fluid Hyperthermia (MFH) of the four samples dispersed in toluene (0.4 wt.%) performed in the DM100-model with amplitude of 16 kA/m and frequency of 570 kHz.

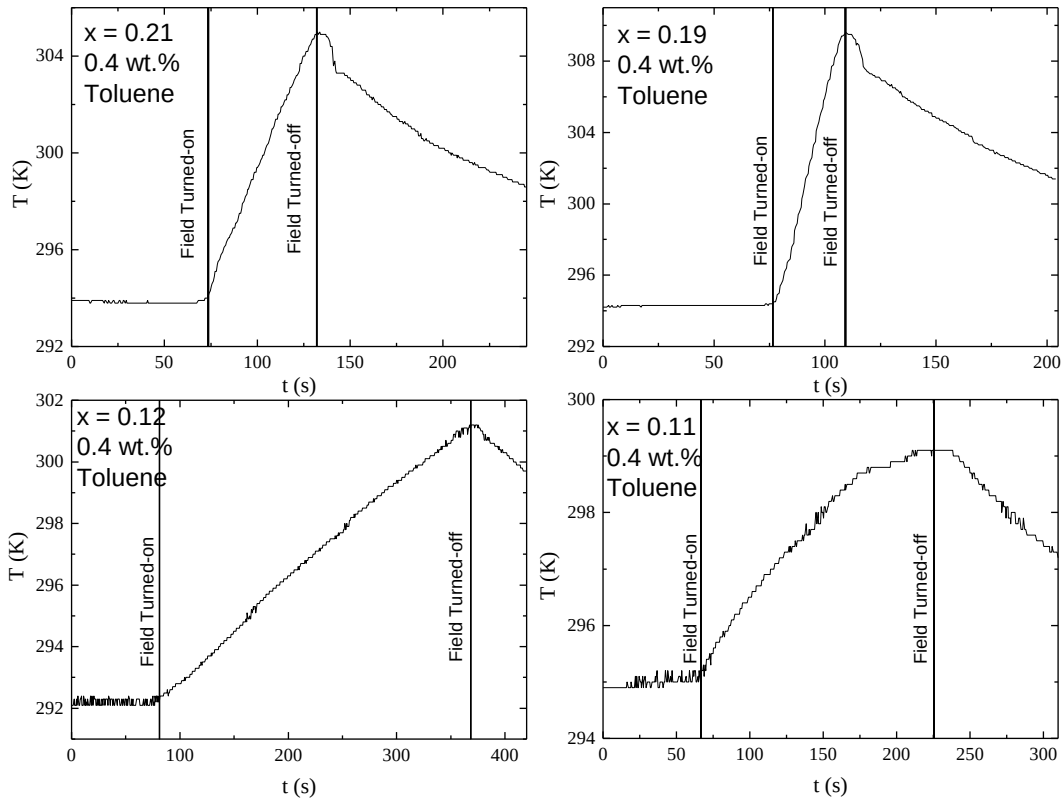

Figure S10: Temperature increment as function of time during MFH experiments of nanoparticles dispersed in toluene.